

Article

Usefulness of Ultrasound Shear Wave Elastography for Detection of Quadriceps Contracture in Immobilized Rats

Kanokwan Suwankanit ^{1,2} , Miki Shimizu ^{1,*} , Kazuhiko Suzuki ³  and Masahiro Kaneda ⁴ 

- ¹ Department of Veterinary Diagnostic Imaging, Faculty of Agriculture, Tokyo University of Agriculture and Technology, 3-5-8 Saiwai-cho, Tokyo 183-0054, Japan; s212485w@st.go.tuat.ac.jp
- ² Department of Clinical Sciences and Public Health, Faculty of Veterinary Science, Mahidol University, Nakhon Pathom 73170, Thailand
- ³ Laboratory of Veterinary Toxicology, Faculty of Agriculture, Tokyo University of Agriculture and Technology, 3-5-8 Saiwai-cho, Tokyo 183-0054, Japan; kzsuzuki@cc.tuat.ac.jp
- ⁴ Laboratory of Veterinary Anatomy, Faculty of Agriculture, Tokyo University of Agriculture and Technology, 3-5-8 Saiwai-cho, Tokyo 183-8509, Japan; kanedam@cc.tuat.ac.jp
- * Correspondence: fx7411@go.tuat.ac.jp; Tel.: +81-42-367-5605

Simple Summary: Quadriceps contracture is a rare disorder that occurs particularly in young animals. Prolonged immobilization of the stifle joint in the extended position is one factor in the development of quadriceps contracture. Clinical diagnostic methods include history taking and physical examination. In most cases, a diagnosis of quadriceps contracture is obtained at an advanced stage of the disease when the prognosis is poor. Therefore, a method for the early clinical detection of quadriceps contracture is needed. We evaluated muscle elastic modulus using ultrasound shear wave elastography, muscle stiffness using a tissue hardness meter, and serum creatinine phosphokinase levels over time in quadriceps contracture model rats and compared their ability to detect pathology. Quadriceps contracture was induced by immobilization of the joints of the hindlimb. During the 4 week immobilization period, in addition to the three clinical examinations, we measured the range of joint motion, histopathology of the muscles, and levels of fibrosis-associated mRNA expression. The elastic modulus increased with the progression of quadriceps contracture, suggesting that ultrasound shear wave elastography is a useful method for the early detection of this disease.



Citation: Suwankanit, K.; Shimizu, M.; Suzuki, K.; Kaneda, M. Usefulness of Ultrasound Shear Wave Elastography for Detection of Quadriceps Contracture in Immobilized Rats. *Animals* **2024**, *14*, 76. <https://doi.org/10.3390/ani14010076>

Academic Editors: Simona Di Pietro and Francesco Macri

Received: 1 November 2023

Revised: 15 December 2023

Accepted: 21 December 2023

Published: 24 December 2023



Copyright: © 2023 by the authors. Licensee MDPI, Basel, Switzerland. This article is an open access article distributed under the terms and conditions of the Creative Commons Attribution (CC BY) license (<https://creativecommons.org/licenses/by/4.0/>).

Abstract: Quadriceps contracture is an abnormal pathological shortening of the muscle–tendon unit. To improve the prognosis of quadriceps contracture, improvement of its diagnostic method is needed. In this study, we evaluated the diagnostic utility of ultrasound shear wave elastography in a rat model of quadriceps contracture induced by immobilization. Fifty Wistar rats were randomly divided into control and immobilization groups. During up to 4 weeks of joint immobilization, the quadriceps elastic modulus, muscle hardness, creatinine phosphokinase levels, joint range of motion, histopathologic parameters, and levels of fibrosis-associated mRNA expression were measured every week in the immobilization and control groups and compared. In the immobilization group, the elastic modulus gradually but significantly increased ($p < 0.05$) throughout the immobilization period. However, muscle hardness and serum creatinine phosphokinase levels only increased at 1 and 2 weeks after the start of immobilization, respectively. Muscle atrophy and shortening progressed throughout the immobilization group. Collagen type I and III, α -SMA protein, and mRNA expression of *IL-1 β* and *TGF- β 1* significantly increased ($p < 0.05$) throughout in the immobilization group. Ultrasound shear wave elastography is the most useful method for clinical assessment of muscle contracture.

Keywords: muscle atrophy; muscle elasticity; muscle stiffness; range of joint motion; sarcomere length

1. Introduction

Quadriceps contracture is characterized by the replacement of the quadriceps muscle–tendon unit with fibrous tissue, resulting in a shortening of the quadriceps muscle, limiting

the range of stifle joint motion, and leading to muscle atrophy and fibrosis [1,2]. The important factor of quadriceps contracture is long-term stifle joint immobilization following orthopedic surgery [3,4]. The prognosis for limb function depends on the degree of quadriceps contracture [3–5]: the earlier the diagnosis, the better the prognosis [2].

The traditional method of diagnosis of quadriceps contracture is history taking and physical examination [1]. Animals with quadriceps contracture present with chronic lameness and a decreased range of stifle joint motion. Blood biochemistry panels tend to be within the normal range, although creatinine phosphokinase levels may be increased [2]. Atrophy of the quadriceps muscle can cause it to feel like a thickened cord when palpated [1,4]. As the disease progresses, the elasticity of the quadriceps muscle decreases and muscle stiffness increases. Therefore, it is desirable to be able to clinically quantify muscle elasticity and thus detect lesions in the quadriceps muscle.

Muscle stiffness, which is defined as the change in muscle resistance to a change in muscle length [6], can be assessed using palpation, a tissue hardness meter [7,8], ultrasound elastography [9–11], or magnetic resonance elastography [12,13]. Palpation is commonly used to evaluate the resistance of muscle; however, it is a subjective assessment. A tissue hardness meter measures the strength of tissue resistance by applying pressure but cannot evaluate individual muscles. Magnetic resonance elastography can provide a larger measurement field than ultrasound and is not limited by muscle depth [14]. It can also quantify muscle stiffness and provide three-dimensional data [13,15]. However, the difficulty of obtaining magnetic resonance equipment, its high cost, and limited use in monitoring quadriceps contracture are major disadvantages [16].

Ultrasound shear wave elastography is a low-invasive, dynamic, and real-time ultrasound imaging technology [17]. Dependent on the shear wave velocity, the Young's modulus elasticity value is calculated, which relies on the use of an ultra-high-speed algorithm [18]. This technique can capture the distribution of stiffness within specific muscles along the direction of the muscle by measuring the elastic modulus (in kilopascals) [18–20]. It produces both a qualitative color-coded shear wave velocity map placing on the B-mode image inside a region of interest [21] and a quantitative evaluation of tissue elasticity [17,22]. The disadvantage is that there are limits to the depth and range of measurements that can be taken [17]. It has been used to investigate the elastic modulus of relaxed and contracted muscles in humans [19]. However, there have been no reports on the use of shear wave elastography to evaluate quadriceps contracture. In this study, three clinical examinations (ultrasound shear wave elastography, tissue hardness meter, and serum creatinine phosphokinase levels) were performed during a period of immobilization of up to 4 weeks in a rat model of quadriceps contracture. The pathophysiology of quadriceps contracture was assessed by the range of joint motion, histopathology, and gene expression levels of *interleukin-1 β* (*IL-1 β*), *transforming growth factor- β 1* (*TGF- β 1*) and *hypoxia-inducible transcription factor-1 α* (*HIF-1 α*). We hypothesized that ultrasound shear wave elastography would be the best method for detecting quadriceps contracture because of its ability to detect changes in muscle elasticity.

2. Materials and Methods

2.1. Animals

Fifty 13 week old, male, specific pathogen-free (SPF) Wistar rats (287.1 ± 12.8) were obtained from Japan SLC International Cooperation, Tokyo, Japan. The animals were maintained in individual cages with dimensions measuring $25 \times 40 \times 20$ cm, with a 12 h light and 12 h dark cycle at a room temperature of 24 ± 2 °C. Food and water were available ad libitum. The experimental protocol was approved by the ethics review committee for animal experimentation at the Tokyo University of Agriculture and Technology (approval number R04-191). Rats were randomly divided into a control group (Group C, $n = 24$) and an immobilization group (Group I, $n = 26$). In each group, the samples were evaluated by equally sampling every other week during the 4 week experimental period (in Group I, weeks 1 and 2, $n = 6$; weeks 3 and 4, $n = 7$).

2.2. Immobilization Procedure

All rats were anesthetized with isoflurane, which was administered using the open drop technique. They were maintained in a correct stage of anesthesia with an anesthetic machine using 1–2% isoflurane with an oxygen flow rate of 300–600 mL/min. For the duration of the anesthesia, the muscles were fully relaxed and did not respond to stimuli; each rat's respiratory rate was maintained at 50–100 bpm. Then the fur on both hindlimbs was clipped. Rats in Group I were immobilized with the stifle joint in full extension and the ankle joint in plantar flexion using a spiral wire immobilization method [23,24]. This method immobilizes the bilateral hindlimbs and is less stressful for the rats than other immobilization methods. To prevent dermatitis, the rats were taped with non-elastic bandage tape (Multipore™ Sports White Athletic Tape, 3M Japan or Kinesio® tape, Tokyo, Japan) to both hindlimbs. A steel bonsai wire (diameter 2.5 mm, length 70 cm) was then applied at the level of the fourth to the fifth lumbar vertebrae and coiled from the hip joints to the end of both hindlimbs. No analgesics or anti-inflammatory drugs were administered during the creation of this model, because no pain or inflammation occurred. The hip joint could move, whereas the stifle and ankle joints could not move. The stifle and ankle joints were immobilized for 1, 2, 3, and 4 weeks. The immobilization procedure was not performed on rats in Group C. The rats were monitored once a day for any sign of bandage loosening or any adverse incidences. The bandages were changed when loosened or an adverse incidence such as hindlimb edema, impaired blood flow at hindlimb, skin injury, or hindlimb necrosis occurred. All of the rats were fitted with vest collars; these were modified versions of the vest collars developed by Jang et al. (2016) [25].

2.3. Joint Angle and Range of Motion Measurement

Flexion and extension angles of the hip, stifle, and ankle joints were measured under anesthesia with isoflurane before and every week during the 4 week experimental period. Joint angles were evaluated using a goniometer according to the method of Millis and Levine (2013) [26]. The range of joint motion was calculated by deducting the flexion angle from the extension angle of that joint.

2.4. Measuring of the Quadriceps Muscle Thickness and Elastic Modulus

Quadriceps thickness and elastic modulus were measured before testing and every week up to 4 weeks during the experimental period. Ultrasonography (LOGIQ-E9 2.0 ultrasound system, GE health care®, Wauwatosa, WI, USA) was performed under anesthesia with isoflurane. The rats were placed in a supine position and the stifle joint angle was set at 135° using a template. Measurements were taken at the quadriceps muscle belly in the right and left limbs. The transducer was set in the vertical direction to the surface of the muscle. Sufficient transmission gel was used to avoid pressure on the muscle by the transducer, to reduce air between the rat skin and the transducer, and to obtain clear images. Echogenicity of muscle fibers is low; perimysium and fascia are highly echogenic.

The thickness of the quadriceps muscle was evaluated by B-mode ultrasound scanning using an L8-18i linear probe (bandwidth: 8–18 MHz; footprint: 35.0 × 7.0 mm). Muscle thickness was defined as the length of a line drawn on a transverse image at 50% of the length of the femur, from the muscle surface to the femur, through the center of the rectus femoris muscle [27,28]. Three measurements were taken, and the mean value was calculated.

Muscle elastic modulus was measured in the rectus femoris, vastus lateralis, and vastus medialis muscle by ultrasound shear wave elastography. The probe (9L linear transducer; bandwidth: 2.5–8 MHz; footprint: 49.0 × 9.0 mm) was applied to the muscle belly, and muscle fibers were delineated parallel to the probe's long axis direction. A square region of interest (1 × 1 cm) was placed within the muscle, and a color-coded elasticity map was displayed in the box in real-time. The scaling of the color display ranged from red to blue, with red indicating high elastic modulus or stiffest tissue and blue indicating low elastic modulus or softest tissue. The fascia and vessel are not included in the region

of interest. A measurement circle range (5 mm in diameter for the rectus femoris and 2 mm in diameter for the vastus lateralis and the vastus medialis muscles) was set at the center of the square region of interest. Five measurements were taken, and the mean value was calculated.

2.5. Measuring Muscle Hardness

Quadriceps hardness was measured using a PEK-MP tissue hardness meter (Imoto Machinery, Tokyo, Japan) before testing and every week during the 4 week experimental period. Stiffness (Newtons, N) is measured on a scale from 0 (soft) to 100 (hard). The rats were placed in a supine position and the stifle joint was extended to 135° [29]. Three measurements were taken at the midpoint of quadriceps of both limbs, and the average value was used for the measurements.

2.6. Evaluation of Creatinine Phosphokinase Level

Creatinine phosphokinase levels were measured weekly during the 4 week experimental period. Blood was collected by cardiac puncture while the rats were alive [30]. Blood was placed in heparin tubes and centrifuged to obtain serum. Creatinine phosphokinase levels were measured on a DRI-CHEM NX700 analyzer (Fujifilm Medical Co., Ltd., Tokyo, Japan).

2.7. Muscle Collection and Measurement

Every week during the 4 week experimental period, rats were euthanized using the open drop technique with 30% isoflurane. Bilateral thoracotomy was performed to confirm cardiac arrest according to the Guide for the Care and Use of Laboratory Animals [31,32]. Then, bilateral quadriceps muscles were excised, wet weight was measured using digital scales and quadriceps muscle weight was standardized by body weight. Muscle size (length × width × height) was measured using a digital caliper.

2.8. Histopathological Examination

The belly of the right quadriceps muscle was cut into a longitudinal section and a cross-section. Both sections were fixed in 4% paraformaldehyde at 4 °C for 36–48 h. These specimens were washed in distilled water and dehydrated in a graded series of ethanol. They were then equilibrated with xylene and embedded in paraffin. Serial cross-sectional and longitudinal 4 µm sections were cut using a microtome and then stained with hematoxylin & eosin (H&E) [33].

A light microscope (Keyence BZ-X800, Keyence Corporation, Osaka, Japan) was used to take photographs for the histological findings at a final magnification of ×400, and ImageJ software version 1.53 (National Institutes of Health, Bethesda, MD, USA) was used to perform the morphological analysis. Sarcomere length was measured by taking 10 longitudinal images per quadriceps muscle, and more than 1000 sarcomeres were randomly selected. Cross-sectional area, minimum Feret's diameter, perimeter, and diameter of muscle fibers were measured by scanning cross-sectional images and randomly selecting 400 muscle fibers.

2.9. Immunohistochemical Analysis

For the immunohistochemical analysis, longitudinal sections of the right quadriceps muscle were deparaffinized in xylene, rehydrated with a graded series of ethanol, and washed in running water. Then, the sections were autoclaved in a target retrieval solution at 121 °C for 10 min. To inhibit endogenous peroxidase activity, the sections were incubated with 1% H₂O₂ in methanol for 30 min at room temperature, before being washed in 0.01 M phosphate-buffered saline (PBS; pH 7.4) and then blocked with 1% normal goat serum for 30 min at room temperature. The sections were incubated overnight at 4 °C with collagen type I monoclonal antibody (COL-1; Invitrogen[®], Carlsbad, CA, USA; diluted ×200), collagen type III monoclonal antibody (FH-7A, Invitrogen[®], Rockford, IL, USA;

diluted $\times 50$), and monoclonal mouse anti-human smooth muscle actin (Clone 1A4, Sigma-Aldrich[®], Glostrup, Denmark; diluted $\times 200$). Then, the sections were rinsed in PBS for 15 min, after which they were incubated with EnVision horseradish peroxidase anti-mouse (Dako EnVision+, HRP, Agilent Technology[®], Santa Clara, CA, USA) for 30 min at room temperature. The sections were rinsed in PBS, and horseradish peroxidase-binding sites were visualized with 0.05% 3,3'-diaminobenzidine and 0.01% H₂O₂ in 0.05 M Tris buffer at room temperature. After a final washing step, the sections were counterstained with hematoxylin. Finally, the sections were dehydrated in increasing concentrations of alcohol, washed with xylene, and mounted on slides. Immunohistochemical analysis of the samples was performed using a light microscope (Keyence BZ-X800, Keyence Corporation, Osaka, Japan) in combination with ImageJ software version 1.53 (National Institutes of Health). The number of myofibroblasts was determined from the images by measuring the α -smooth muscle actin (α -SMA)-positive cells. The number of α -SMA-positive cells was counted in all fields for each section at $\times 200$ magnification, and the average number per field was calculated. The levels of collagen types I and III were determined using a semi-quantitative technique. The percentage of collagen to total tissue longitudinal area, including the muscle, perivascular, and interstitial areas, was calculated for the total slide area at $\times 200$ magnification. Areas of muscle overlap or poor staining were excluded. All analyses were performed under conditions where the analyst was blinded to the experimental group to which the slides belonged.

2.10. Real-Time RT-PCR to Measure Interleukin-1 β (IL-1 β), Transforming Growth Factor- β 1 (TGF- β 1), and Hypoxia-Inducible Transcription Factor-1 α (HIF-1 α) mRNA

The left quadriceps muscle was used for real-time RT-PCR analysis. Total RNA was extracted from the muscle samples using TRIzol reagent (TRIzol[™], Invitrogen[®], Carlsbad, CA, USA), according to the manufacturer's protocol. Total RNA was used as a template with the qPCR RT Master Mix (ReverTra Ace, Toyobo Co., Ltd., Osaka, Japan) to prepare cDNA. The mRNA expression levels were then determined using real-time RT-PCR, which was performed in an optical 96 well plate with the StepOnePlus[™] Real-Time PCR System (Applied BioSystems, Foster City, CA, USA). The primer sequences used for the real-time RT-PCR are shown in Table 1. Relative quantification was calculated using the $2^{-\Delta\Delta C_t}$ method [34] and normalized to β -actin. Data are presented as expression levels relative to the expression level in the control group.

Table 1. Sequences of primers used for the real-time RT-PCR.

Object Gene	F/R	Sequence
IL-1 β	F	5'-AATGACCTGTTCTTTGAGGCTGAC-3'
	R	5'-CGAGATGCTGCTGTGAGATTTGAA-3'
TGF- β 1	F	5'-ATGCCAACTTCTGTCTGGGG-3'
	R	5'-GGTTGTAGAGGGCAAGGACC-3'
HIF-1 α	F	5'-TGCTGGCTCCCTATATCCCA-3'
	R	5'-GGAGGGCTTGGAGAATTGCT-3'
β -actin	F	5'-GCAGGAGTACGATGAGTCCG-3'
	R	5'-ACGCAGCTCAGTAACAGTCC-3'

F, forward; R, reverse.

2.11. Statistical Analysis

GraphPad Prism version 8 (GraphPad Software Inc., San Diego, CA, USA) was used to perform the statistical analysis. All data are presented as mean and standard deviation. Comparisons between control and immobilization groups in the same period were performed using the Mann–Whitney test, while differences in each period within the same group were assessed using the Kruskal–Wallis test, followed by Dunn's multiple comparison test. Statistical significance was set at $p < 0.05$.

3. Results

3.1. Joint Angle and Range of Motion (ROM)

The measured angles of maximum extension, maximum flexion, and range of motion of the hip, stifle, and ankle joints are shown in Table 2. There was no significant difference in the range of motion of the hip joint between Group C and Group I for each period. In Group I, the stifle and ankle flexion angles of Group I increased ($p = 0.0001$) and the range of motion of both joints decreased ($p = 0.0001$). The range of motion of the stifle and ankle joints in Group I at 3 and 4 weeks after immobilization was decreased compared to Group I at 1 week.

Table 2. Joint angle ($^{\circ}$) and ROM of rats in the control and immobilization groups.

Joint and Position		Duration	Group C	Group I	
Hip	Extension	Pre	156 ± 3.2 ($n = 48$)	157 ± 3.3 ($n = 52$)	
		1 week	155 ± 2.3 ($n = 12$)	156 ± 3.1 ($n = 12$)	
		2 weeks	155 ± 1.4 ($n = 12$)	156 ± 1.9 ($n = 12$)	
		3 weeks	156 ± 1.7 ($n = 12$)	156 ± 1.4 [#] ($n = 14$)	
	Flexion	4 weeks	156 ± 2.2 ($n = 12$)	157 ± 2.5 ($n = 14$)	
		Pre	30 ± 1.6 ($n = 48$)	31 ± 2.0 ($n = 52$)	
		1 week	30 ± 1.0 ($n = 12$)	30 ± 0.6 ($n = 12$)	
		2 weeks	30 ± 0.8 ($n = 12$)	31 ± 1.7 ($n = 12$)	
	ROM	3 weeks	30 ± 0.9 ($n = 12$)	30 ± 1.3 ($n = 14$)	
		4 weeks	30 ± 0.6 ($n = 12$)	31 ± 4.0 ($n = 14$)	
		Pre	126 ± 3.3 ($n = 48$)	127 ± 3.4 ($n = 52$)	
		1 week	126 ± 2.4 ($n = 12$)	126 ± 3.2 ($n = 12$)	
	Stifle	Extension	2 weeks	126 ± 1.5 ($n = 12$)	126 ± 2.5 ($n = 12$)
			3 weeks	127 ± 1.8 ($n = 12$)	125 ± 2.0 ($n = 14$)
			4 weeks	127 ± 2.6 ($n = 12$)	126 ± 3.9 ($n = 14$)
			Pre	164 ± 2.4 ($n = 48$)	164 ± 2.5 ($n = 52$)
Flexion		1 week	162 ± 2.4 [#] ($n = 12$)	162 ± 3.2 [#] ($n = 12$)	
		2 weeks	164 ± 2.0 ($n = 12$)	162 ± 2.5 [#] ($n = 12$)	
		3 weeks	162 ± 2.3 [#] ($n = 12$)	161 ± 2.1 [#] ($n = 14$)	
		4 weeks	163 ± 2.4 ($n = 12$)	163 ± 2.5 ($n = 14$)	
ROM		Pre	30 ± 1.3 ($n = 48$)	30 ± 2.0 ($n = 52$)	
		1 week	30 ± 0.8 ($n = 12$)	50 ± 8.4 ^{*#} ($n = 12$)	
		2 weeks	30 ± 0.3 ($n = 12$)	72 ± 11.8 ^{*#} ($n = 12$)	
		3 weeks	30 ± 0.0 ($n = 12$)	96 ± 7.5 ^{*#a} ($n = 14$)	
Ankle		Extension	4 weeks	30 ± 0.0 ($n = 12$)	112 ± 7.9 ^{*#ab} ($n = 14$)
			Pre	134 ± 2.8 ($n = 48$)	134 ± 3.3 ($n = 52$)
			1 week	132 ± 2.6 ($n = 12$)	112 ± 8.4 ^{*#} ($n = 12$)
			2 weeks	134 ± 2.1 ($n = 12$)	89 ± 11.1 ^{*#} ($n = 12$)
	Flexion	3 weeks	132 ± 2.3 [#] ($n = 12$)	66 ± 6.9 ^{*#a} ($n = 14$)	
		4 weeks	133 ± 2.4 ($n = 12$)	52 ± 8.1 ^{*#ab} ($n = 14$)	
		Pre	167 ± 2.6 ($n = 48$)	167 ± 3.2 ($n = 52$)	
		1 week	169 ± 1.5 [#] ($n = 12$)	168 ± 3.3 ($n = 12$)	
Ankle	Extension	2 weeks	168 ± 2.4 ($n = 12$)	170 ± 2.6 [#] ($n = 12$)	
		3 weeks	168 ± 2.5 ($n = 12$)	169 ± 2.1 [#] ($n = 14$)	
		4 weeks	170 ± 1.9 [#] ($n = 12$)	170 ± 1.8 [#] ($n = 14$)	
		Pre	10 ± 1.3 ($n = 48$)	10 ± 1.4 ($n = 52$)	
	Flexion	1 week	10 ± 0.8 ($n = 12$)	62 ± 14.7 ^{*#} ($n = 12$)	
		2 weeks	9 ± 1.1 ($n = 12$)	84 ± 13.9 ^{*#} ($n = 12$)	
		3 weeks	10 ± 0.6 ($n = 12$)	106 ± 6.9 ^{*#a} ($n = 14$)	
		4 weeks	10 ± 0.4 ($n = 12$)	130 ± 11.2 ^{*#ab} ($n = 14$)	
ROM	Pre	158 ± 2.6 ($n = 48$)	158 ± 3.5 ($n = 52$)		
	1 week	160 ± 1.3 [#] ($n = 12$)	106 ± 13.7 ^{*#} ($n = 12$)		
	2 weeks	159 ± 2.4 ($n = 12$)	86 ± 13.6 ^{*#} ($n = 12$)		
	3 weeks	159 ± 2.3 ($n = 12$)	63 ± 7.6 ^{*#a} ($n = 14$)		
4 weeks	160 ± 2.1 [#] ($n = 12$)	40 ± 11.3 ^{*#ab} ($n = 14$)			

Values are expressed as mean and standard deviation. Group C, control group; Group I, immobilization group; Pre, before the experiment; * significantly different from Group C in the same period and the same position of the joint ($p < 0.0001$); # significantly different from Pre in the same group and the same position of the joint ($p < 0.05$); ^a significantly different from the 1 week period in the same group and the same position of the joint ($p < 0.001$); ^b significantly different from the 2 week period in the same group and the same position of the joint ($p < 0.05$).

3.2. Measurement of Thigh Muscle Thickness

Representative measurements of thigh muscle thickness are shown in Figure 1. The hypoechogenicity of muscle fibers and hyperechogenicity of perimysium and fascia were observed.

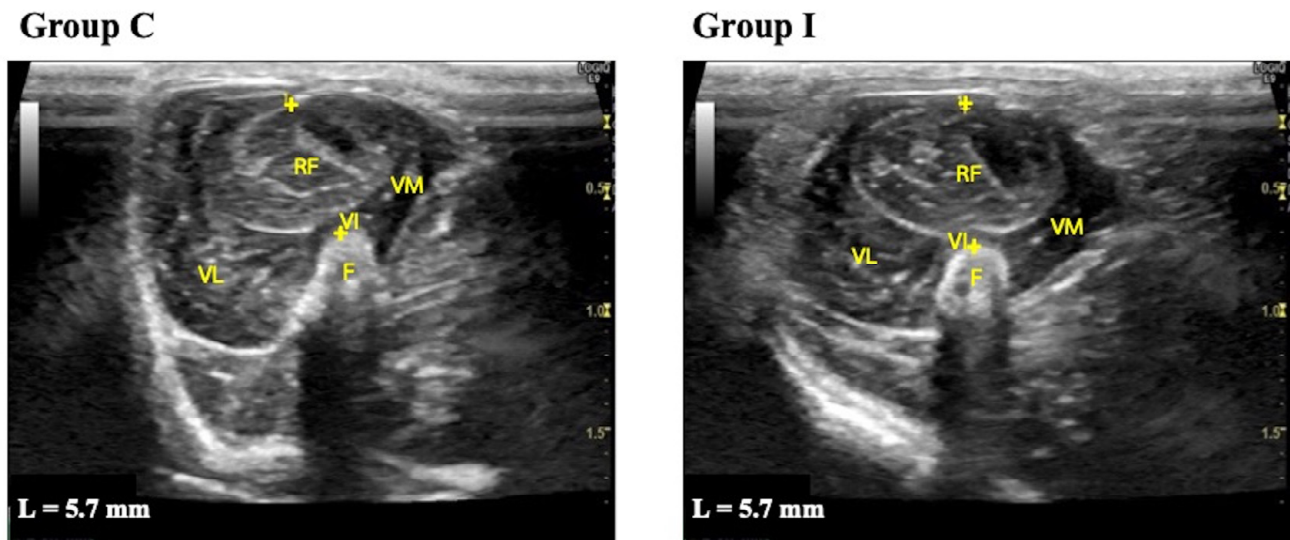


Figure 1. Representative transverse B-mode ultrasound images of the quadriceps muscle used to measure muscle thickness before the experiment. Group C, control group; Group I, immobilization group; L, thigh muscle thickness. F: femur; RF: rectus femoris; VL: vastus lateralis; VM: vastus medialis; VI: vastus intermedius; +: electronic caliper. The images show the placement of the electronic calipers to measure the cross-section at 50% of the femur length by passing across the center of the rectus femoris muscle from the surface of the muscle to the femoral bone.

The measurements of quadriceps muscle thicknesses are shown in Table 3. The quadriceps muscle thickness in Group I was decreased in all periods compared to Group C. In Group C, on the other hand, the quadriceps muscle thickness increased as the rats grew.

Table 3. Quadriceps muscle thickness measurements (mm).

Duration	Group C	Group I
Pre	5.6 ± 0.3 (n = 48)	5.7 ± 0.4 (n = 52)
1 week	5.6 ± 0.3 (n = 12)	4.8 ± 0.4 ^{*#} (n = 12)
2 weeks	5.8 ± 0.3 [#] (n = 12)	4.7 ± 0.4 ^{*#} (n = 12)
3 weeks	5.9 ± 0.3 [#] (n = 12)	4.5 ± 0.2 ^{*#} (n = 12)
4 weeks	6.1 ± 0.2 ^{#a} (n = 12)	4.5 ± 0.3 ^{*#} (n = 14)

Values are expressed as mean and standard deviation. Group C, control group; Group I, immobilization group; Pre, before the experiment; * significantly different from Group C in the same period ($p < 0.0001$); # significantly different from Pre in the same group ($p < 0.05$); ^a significantly different from the 1 week period in the same group ($p < 0.001$).

3.3. Elastic Modulus

Representative longitudinal ultrasound shear wave elastography images of the rectus femoris, vastus lateralis, and vastus medialis muscle are shown in Figure 2, Figure 3, and Figure 4, respectively. In Group I, cyan, orange, and red colors increased during the immobilization period, suggesting an increased elastic modulus.

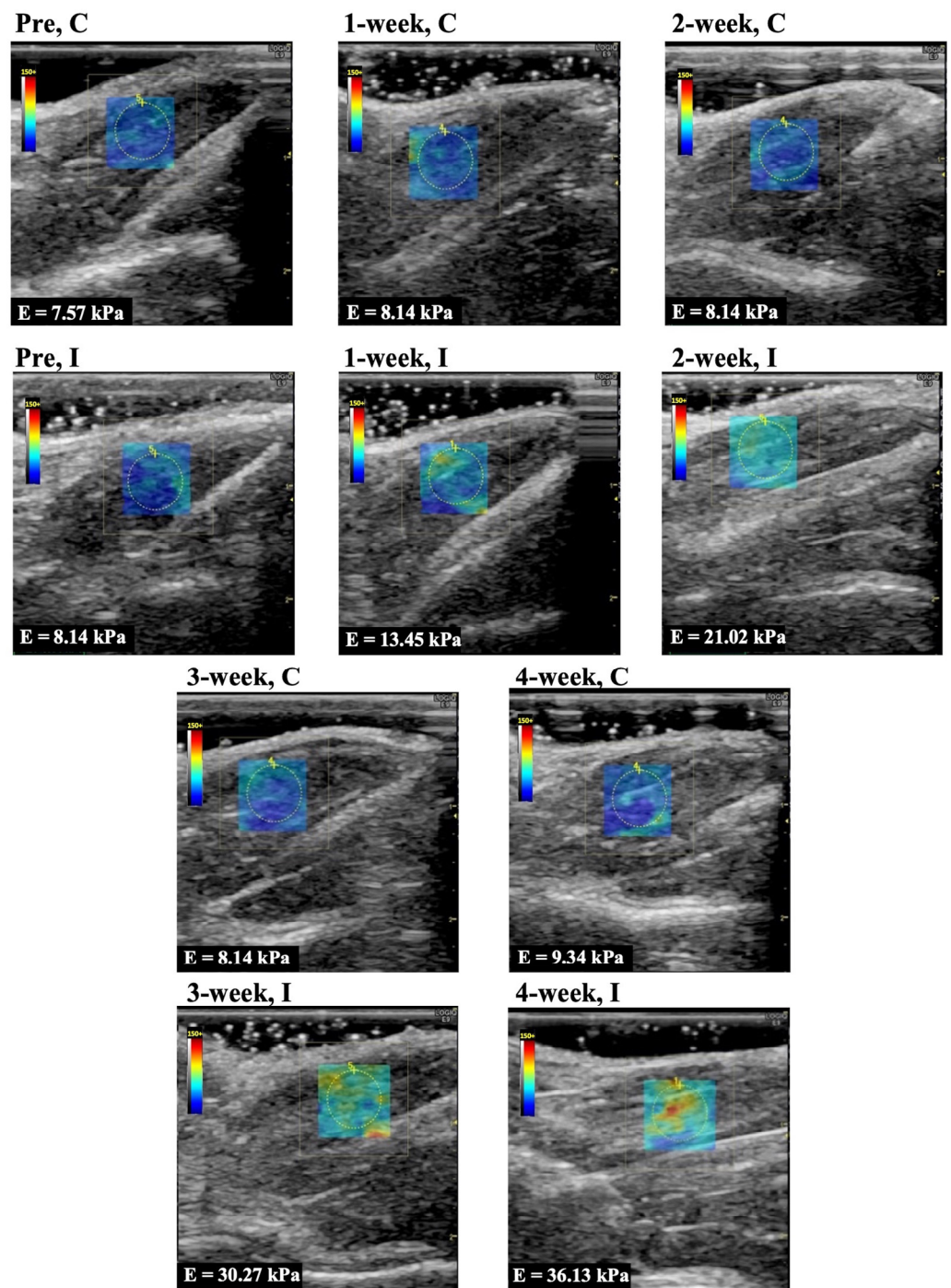


Figure 2. Representative shear wave elastography of the rectus femoris muscle. C, control group; I, immobilization group; Pre, before the experiment; E, elastic modulus. The rectangle indicates the region of interest. The measurement circle was 5 mm in diameter.

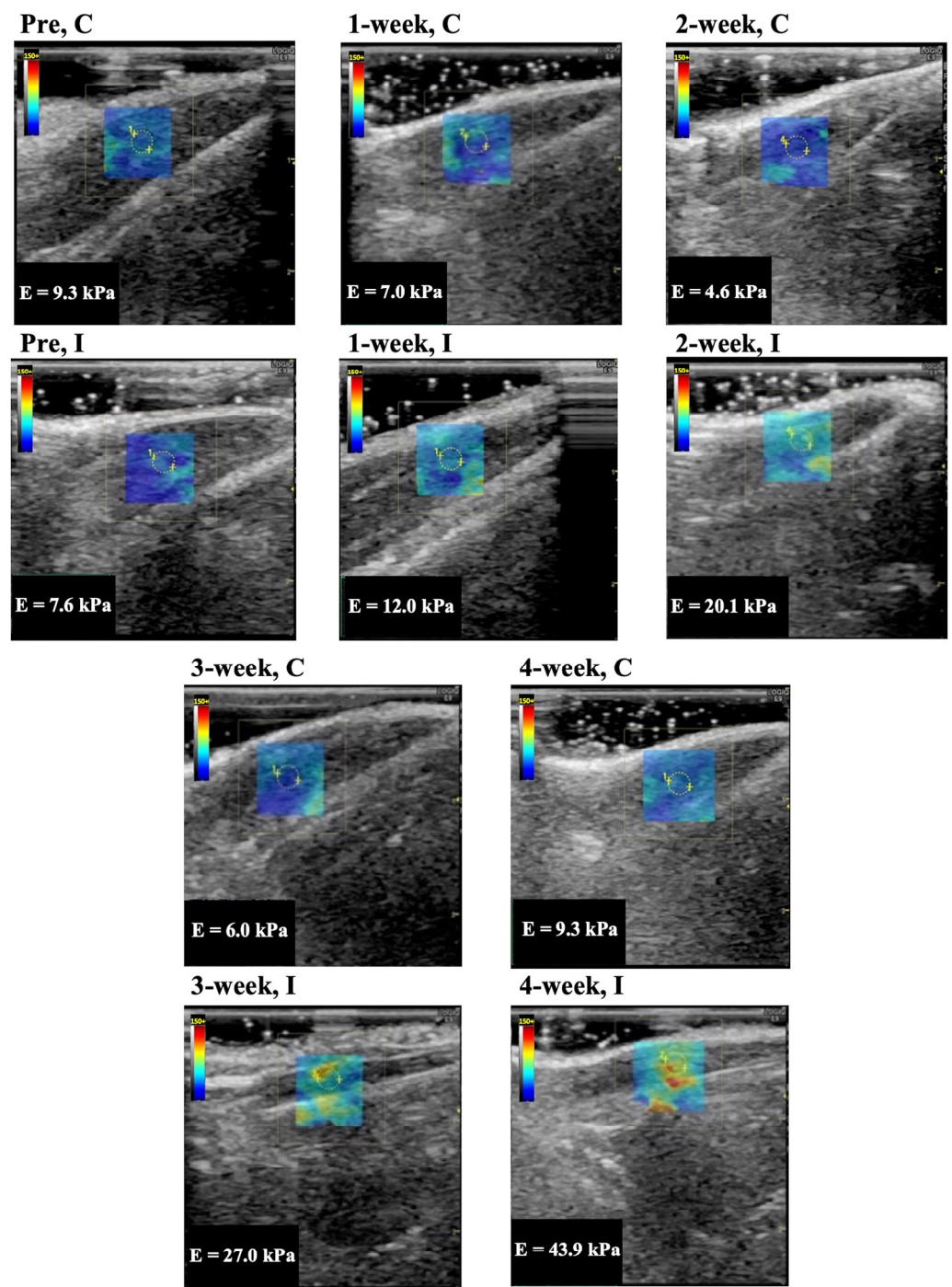


Figure 3. Representative shear wave elastography of the vastus lateralis muscle. C, control group; I, immobilization group; Pre, before the experiment; E, elastic modulus. The rectangle indicates the region of interest. The measurement circle was 2 mm in diameter.

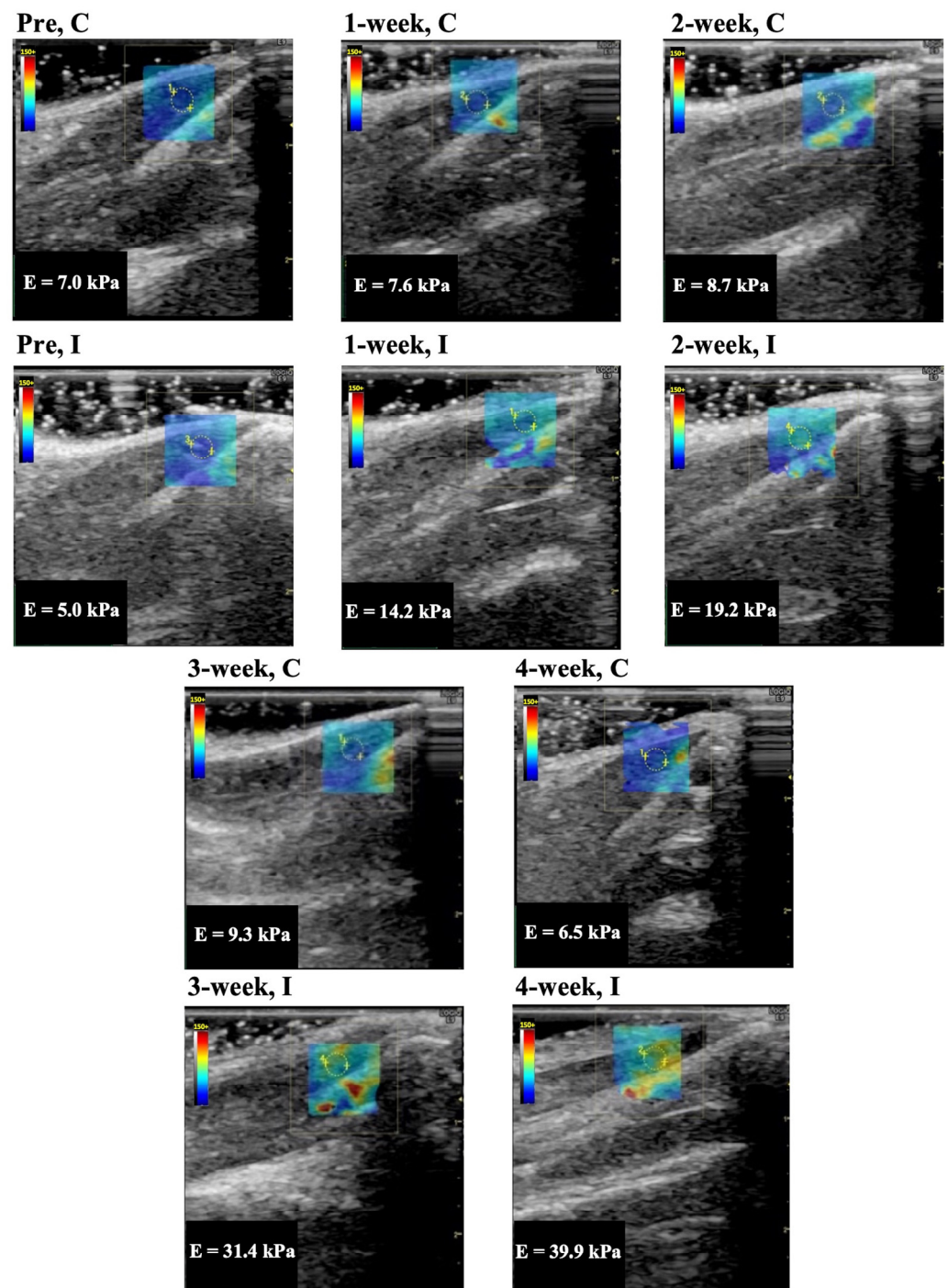


Figure 4. Representative shear wave elastography of the vastus medialis muscle. C, control group; I, immobilization group; pre, before the experiment; E, elastic modulus. The rectangle indicates the region of interest. The measurement circle was 2 mm in diameter.

The elastic modulus of the rectus femoris, vastus lateralis, and vastus medialis muscle as determined by ultrasound shear wave elastography are shown in Figure 5A–C. The elastic modulus of the rectus femoris, vastus lateralis, and vastus medialis muscles in Group C were 8.6 ± 1.0 , 7.4 ± 1.3 , 7.6 ± 1.1 kPa (mean and standard deviation) in before experiment, 7.5 ± 1.4 , 7.8 ± 0.8 , 8.7 ± 0.5 kPa in 1 week, 7.4 ± 1.2 , 7.1 ± 1.6 , 8.0 ± 1.5 kPa in 2 weeks, 8.6 ± 1.2 , 7.5 ± 0.9 , 8.4 ± 0.7 kPa in 3 weeks, and 8.0 ± 1.0 , 7.4 ± 1.0 , 8.5 ± 0.7 kPa in 4 weeks, respectively. The elastic modulus of those muscles in Group I was 8.3 ± 1.2 , 7.4 ± 1.1 , 7.7 ± 1.1 kPa in the before experiment, 15.0 ± 1.4 , 15.2 ± 2.2 , 14.5 ± 1.5 kPa in

1 week, 20.1 ± 1.7 , 19.6 ± 2.2 , 18.9 ± 2.5 kPa in 2 weeks, 29.0 ± 2.1 , 28.8 ± 1.7 , 29.2 ± 2.4 kPa in 3 weeks, and 30.6 ± 2.7 , 32.9 ± 4.0 , 33.1 ± 3.4 kPa in 4 weeks, respectively. The elastic modulus for all periods in Group I was significantly higher ($p = 0.0001$ in all muscles) compared with the same periods in Group C. In Group I, the elastic modulus increased after more than 3 weeks of immobilization compared to the 1 and 2 week immobilizations.

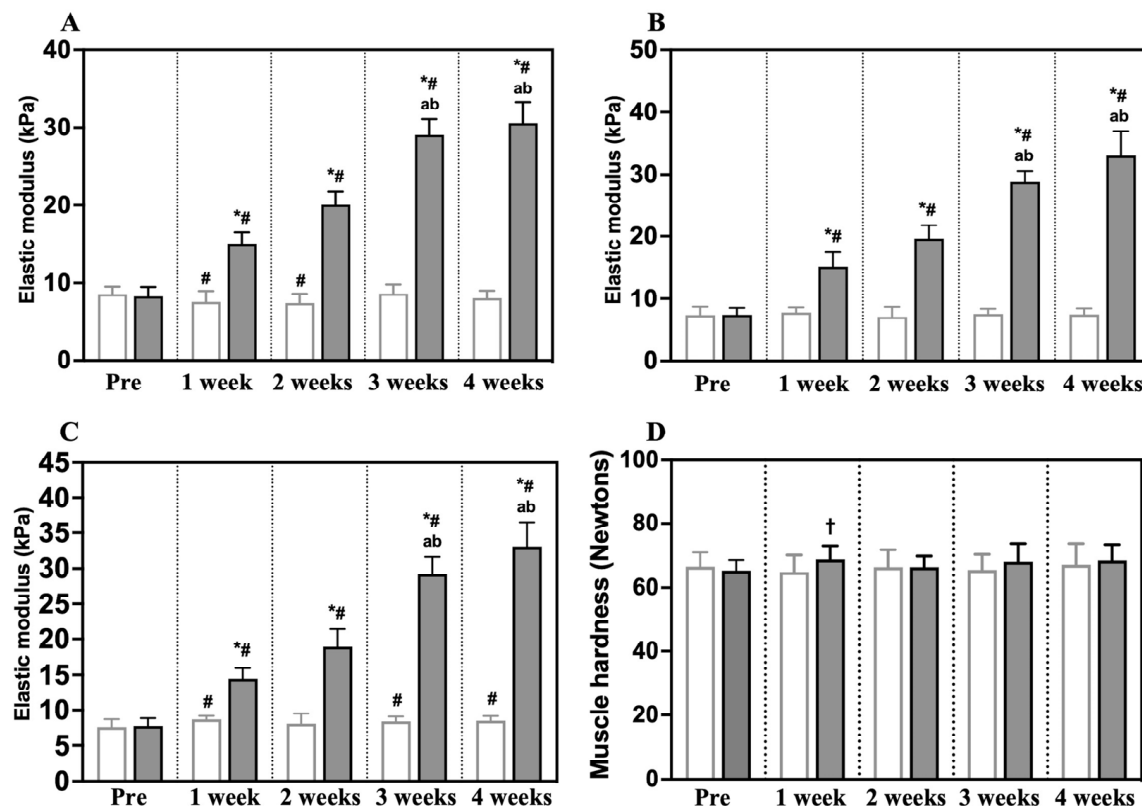


Figure 5. The elastic modulus of the rectus femoris (A), vastus lateralis (B), and vastus medialis muscles (C), measured by ultrasound shear wave elastography; and the quadriceps muscle hardness (D), measured using a tissue hardness meter. The empty (white) bars show Group C (control group); the gray bars show Group I (immobilization group); Pre, before the experiment; * significantly different from Group C in the same period ($p < 0.0001$); † significantly different from Group C in the same period ($p < 0.05$); # significantly different from Pre in the same group ($p < 0.05$); ^a significantly different from the 1 week period in the same group ($p < 0.001$); ^b significantly different from the 2 week period in the same group ($p < 0.05$). Values shown are mean and standard deviation.

3.4. Muscle Hardness

The quadriceps muscle hardness values are shown in Figure 5D. The quadriceps muscle hardness of Group C and Group I were 67 ± 4.3 and 65 ± 3.2 N (mean and standard deviation) before the experiment, 65 ± 5.1 and 69 ± 4.2 N in 1 week, 66 ± 5.3 and 66 ± 3.3 N in 2 weeks, 66 ± 4.7 and 68 ± 5.6 N in 3 weeks, and 67 ± 6.5 and 68 ± 4.9 N in 4 weeks. The hardness value of the quadriceps muscles was only higher in Group I compared with Group C in week 1 ($p = 0.0424$).

3.5. Creatinine Phosphokinase Level

The creatinine phosphokinase levels are shown in Table 4. In Group I, the level of creatinine phosphokinase increased at 2 weeks compared with Group C in the same period ($p = 0.0152$).

Table 4. Creatinine phosphokinase level (U/L).

Duration	Group C	Group I
1 week	345 ± 157 (n = 6)	460 ± 383 (n = 6)
2 weeks	259 ± 86 (n = 6)	475 ± 112 * (n = 6)
3 weeks	473 ± 292 (n = 6)	493 ± 339 (n = 7)
4 weeks	237 ± 99 (n = 6)	279 ± 102 (n = 7)

Values are expressed as mean and standard deviation. Group C, control group; Group I, immobilization group; * significantly different from Group C in the same period ($p < 0.05$).

3.6. The Ratio of Muscle Weight to Body Weight and Quadriceps Muscle Measurement

The ratio of muscle weight to body weight and the length, width, and height of quadriceps muscles are shown in Table 5. These measurements were lower in Group I compared with Group C in the same time periods.

Table 5. Weight and dimensions of quadriceps muscle.

Quadriceps Muscle	1 Week	2 Weeks	3 Weeks	4 Weeks
Muscle weight/body weight (mg/g)				
Group C	8.3 ± 0.4 (n = 12)	7.9 ± 0.2 (n = 12)	8.4 ± 0.2 ^b (n = 12)	8.2 ± 0.3 (n = 12)
Group I	7.6 ± 0.9 * (n = 12)	6.1 ± 0.5 ^{*a} (n = 12)	6.0 ± 0.3 ^{*a} (n = 14)	5.9 ± 0.7 ^{*a} (n = 14)
Muscle length (mm)				
Group C	29.6 ± 1.8 (n = 12)	28.9 ± 1.0 (n = 12)	29.8 ± 1.4 (n = 12)	31.1 ± 2.0 ^b (n = 12)
Group I	25.7 ± 1.8 * (n = 12)	22.9 ± 1.0 ^{*a} (n = 12)	23.0 ± 1.2 ^{*a} (n = 14)	22.3 ± 0.8 ^{*a} (n = 14)
Muscle width (mm)				
Group C	14.3 ± 0.7 (n = 12)	14.1 ± 0.9 (n = 12)	14.6 ± 1.4 (n = 12)	15.2 ± 0.9 (n = 12)
Group I	12.4 ± 0.7 * (n = 12)	11.7 ± 1.1 * (n = 12)	11.5 ± 0.9 * (n = 14)	11.3 ± 1.1 ^{*a} (n = 14)
Muscle height (mm)				
Group C	11.6 ± 1.1 (n = 12)	12.0 ± 1.7 (n = 12)	12.1 ± 1.1 (n = 12)	11.7 ± 1.2 (n = 12)
Group I	10.7 ± 1.2 (n = 12)	9.0 ± 1.8 ^{*a} (n = 12)	8.8 ± 0.6 ^{*a} (n = 14)	8.7 ± 0.5 ^{*a} (n = 14)

Values are expressed as mean and standard deviation. Group C, control group; Group I, immobilization group; * significantly different from Group C in the same period ($p < 0.0001$); ^a significantly different from the 1 week period in the same group ($p < 0.05$); ^b significantly different from the 2 week period in the same group ($p < 0.05$).

3.7. Histological Evaluation of Quadriceps Muscle Fiber and Sarcomere Length

Histological findings of the quadriceps muscle cross-sections stained with H&E for all groups showed a normal microanatomic arrangement, with no lesions of note in the muscle fibers and no inflammatory cells between the muscle bundles. In Group I, the muscle bundles were separated as muscle fascicles surrounded by disorganized and thickened connective tissue in the perimysium and endomysium.

The data for the cross-sectional area, minimum Feret's diameter, diameter, perimeter, and sarcomere length of the quadriceps muscles is shown in Table 6. The cross-sectional area, minimum Feret's diameter, diameter, and perimeter of Group I decreased ($p = 0.0001$) compared with these values for Group C in the same period and showed a gradual decrease ($p = 0.0001$) with increasing immobilization time. The sarcomere length in Group I was lower ($p = 0.0001$) compared with Group C in the same period and decreased as the immobilization period increased.

Table 6. Cross-sectional area, minimum Feret's diameter, diameter, perimeter, and sarcomere length of quadriceps muscles analyzed using H&E staining.

Quadriceps Muscle	1 Week	2 Weeks	3 Weeks	4 Weeks
Cross-sectional area (μm^2)				
Group C	2586 \pm 561 ($n = 2400$)	3907 \pm 688 ^a ($n = 2400$)	4401 \pm 624 ^{ab} ($n = 2400$)	4619 \pm 748 ^{abc} ($n = 2400$)
Group I	2236 \pm 500 * ($n = 2400$)	1237 \pm 336 ^{aa} ($n = 2400$)	1091 \pm 290 ^{ab} ($n = 2800$)	1029 \pm 271 ^{abc} ($n = 2800$)
Minimum Feret's diameter (μm)				
Group C	57.9 \pm 6.8 ($n = 2400$)	59.7 \pm 7.4 ^a ($n = 2400$)	63.4 \pm 7.1 ^{ab} ($n = 2400$)	65.7 \pm 7.6 ^{abc} ($n = 2400$)
Group I	45.4 \pm 6.5 * ($n = 2400$)	33.4 \pm 5.7 ^{aa} ($n = 2400$)	31.8 \pm 5.3 ^{ab} ($n = 2800$)	31.1 \pm 4.9 ^{abc} ($n = 2800$)
Diameter (μm)				
Group C	67.4 \pm 5.2 ($n = 2400$)	70.3 \pm 6.1 ^a ($n = 2400$)	74.7 \pm 5.3 ^{ab} ($n = 2400$)	76.4 \pm 6.2 ^{abc} ($n = 2400$)
Group I	53.0 \pm 5.9 * ($n = 2400$)	39.3 \pm 5.4 ^{aa} ($n = 2400$)	37.0 \pm 4.9 ^{ab} ($n = 2800$)	35.9 \pm 4.7 ^{abc} ($n = 2800$)
Perimeter (μm)				
Group C	235.8 \pm 21.6 ($n = 2400$)	242.2 \pm 23.2 ^a ($n = 2400$)	254.1 \pm 21.7 ^{ab} ($n = 2400$)	258.3 \pm 24.5 ^{abc} ($n = 2400$)
Group I	184.3 \pm 21.5 * ($n = 2400$)	136.6 \pm 19.3 ^{aa} ($n = 2400$)	128.7 \pm 17.9 ^{ab} ($n = 2800$)	121.9 \pm 17.0 ^{abc} ($n = 2800$)
Sarcomere length (nm)				
Group C	1559 \pm 144 ($n = 6000$)	1671 \pm 154 ^a ($n = 6000$)	1673 \pm 127 ^a ($n = 6000$)	1699 \pm 128 ^{abc} ($n = 6000$)
Group I	1415 \pm 146 * ($n = 6000$)	1267 \pm 121 ^{aa} ($n = 6000$)	1137 \pm 105 ^{ab} ($n = 7000$)	1123 \pm 93 ^{abc} ($n = 7000$)

Values are expressed as mean and standard deviation. Group C, control group; Group I, immobilization group; * significantly different from Group C in the same period ($p < 0.0001$); ^a significantly different from 1 week in the same group ($p < 0.05$); ^b significantly different from the 2 week period in the same group ($p < 0.05$); ^c significantly different from the 3 week period in the same group ($p < 0.05$).

3.8. Measurement of α -Smooth Muscle Actin (α -SMA) Cells and Collagen Types I and III

The number of α -SMA-positive cells and the percentage of collagen types I and III are shown in Table 7. These measurements in Group I were significantly higher than those in Group C in the same period and increased as the immobilization period increased.

Table 7. Number of α -smooth muscle actin (α -SMA)-positive cells and the percentage of collagen type I and III in quadriceps muscles of rats in the control and immobilization groups, based on the immunohistochemistry analyses.

Quadriceps Muscle	1 Week	2 Weeks	3 Weeks	4 Weeks
α -SMA (number of cells/field)				
Group C	1.7 \pm 0.2 ($n = 6$)	1.5 \pm 0.1 ($n = 6$)	1.6 \pm 0.3 ($n = 6$)	1.5 \pm 0.3 ($n = 6$)
Group I	5.1 \pm 0.7 * ($n = 6$)	5.5 \pm 0.4 * ($n = 6$)	8.2 \pm 0.7 ^{aa} ($n = 7$)	8.7 \pm 1.2 ^{ab} ($n = 7$)
Collagen type I (%)				
Group C	0.27 \pm 0.10 ($n = 6$)	0.20 \pm 0.09 ($n = 6$)	0.21 \pm 0.10 ($n = 6$)	0.17 \pm 0.05 ($n = 6$)
Group I	1.09 \pm 0.29 * ($n = 6$)	1.63 \pm 0.17 * ($n = 6$)	2.70 \pm 0.37 ^{aa} ($n = 7$)	3.74 \pm 0.30 ^{ab} ($n = 7$)
Collagen type III (%)				
Group C	0.06 \pm 0.02 ($n = 6$)	0.06 \pm 0.01 ($n = 6$)	0.06 \pm 0.01 ($n = 6$)	0.05 \pm 0.00 ($n = 6$)
Group I	0.80 \pm 0.07 * ($n = 6$)	1.28 \pm 0.08 * ($n = 6$)	1.89 \pm 0.09 * ($n = 7$)	2.51 \pm 0.24 ^{ab} ($n = 7$)

Values are expressed as mean and standard deviation. Group C, control group; Group I, immobilization group; * significantly different from Group C in the same period ($p < 0.05$). ^a significantly different from the 1 week period in the same group ($p < 0.05$); ^b significantly different from the 2 week period in the same group ($p < 0.05$).

3.9. Relative Expression of $IL-1\beta$, $TGF-\beta1$, and $HIF-1\alpha$ mRNA

The expression levels of $IL-1\beta$, $TGF-\beta1$, and $HIF-1\alpha$ mRNA in the quadriceps muscle are shown in Figure 6. $IL-1\beta$ mRNA expression in Group I in the 1, 2, 3, and 4 week periods was 3.4 \pm 0.8 fold, 2.7 \pm 1.6 fold, 2.4 \pm 0.8 fold, and 2.7 \pm 1.3 fold (mean and standard deviation) higher, respectively, compared with the levels in Group C in the same periods (Figure 6A). $TGF-\beta1$ mRNA expression in the 1, 2, 3, and 4 week periods was 1.6 \pm 0.3 fold, 1.9 \pm 0.8 fold, 2.3 \pm 1.1 fold, and 2.4 \pm 1.5 fold higher, respectively, compared with the levels in Group C in the same periods (Figure 6B). $HIF-1\alpha$ mRNA expression in Group I in the 1, 2, 3, and 4 week periods was 1.0 \pm 0.2 fold, 1.0 \pm 0.2 fold, 1.1 \pm 0.3 fold, and 1.8 \pm 0.5 fold, respectively, compared with the levels in Group C in the same periods (Figure 6C). In Group I, the expression levels of $IL-1\beta$ and $TGF-\beta1$ mRNA were significantly higher than those in Group C in each of the time periods. The expression level of $HIF-1\alpha$ mRNA in Group I at 4 weeks after immobilization was significantly higher than the other measurement periods in Group I and Group C in the same period.

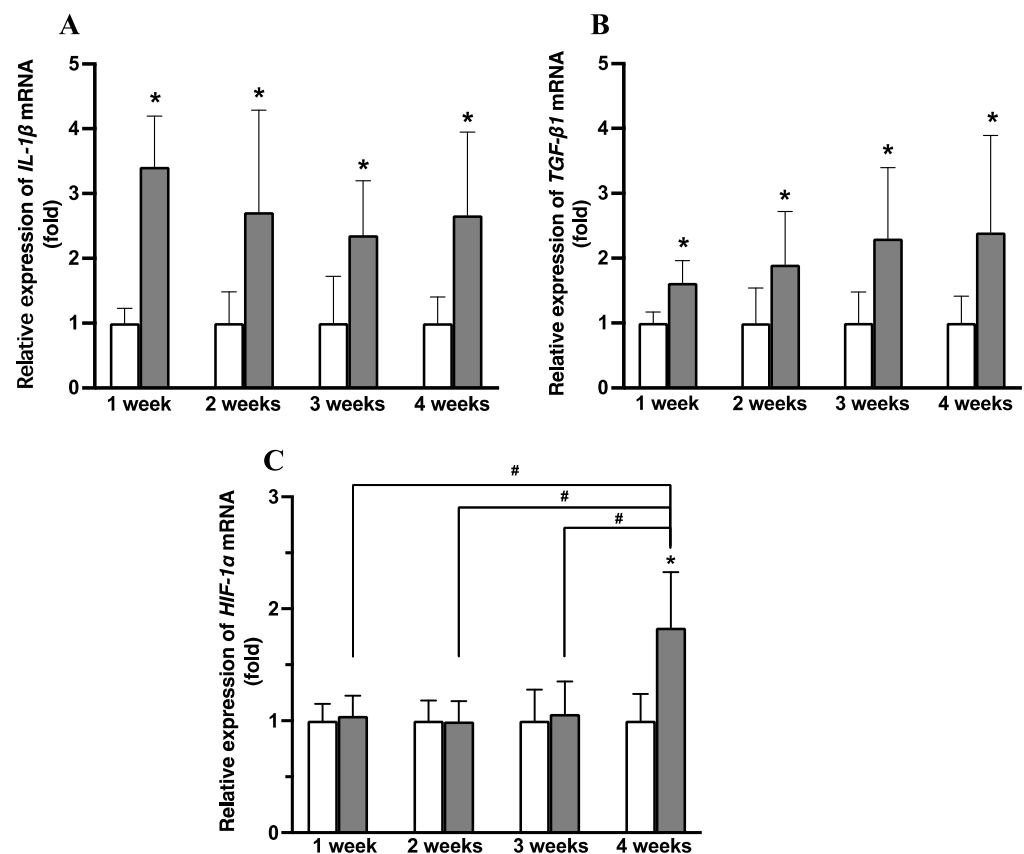


Figure 6. Expression levels of *IL-1 β* (A), *TGF- β 1* (B), and *HIF-1 α* (C) mRNA. The open (white) bars show the control groups, and the gray bars show the immobilization groups. Values are expressed as mean and standard deviation. * Significantly different from Group C in the same period ($p < 0.05$); # significantly different between periods in the immobilization group ($p < 0.05$).

4. Discussion

We evaluated the effectiveness of ultrasound shear wave elastography and the measurement of muscle hardness and creatinine phosphokinase level to diagnose quadriceps muscle contracture by comparing each of them with the pathogenesis of quadriceps contracture. After immobilization for 1, 2, 3, and 4 weeks, the elastic modulus of three muscles in the quadriceps group, the rectus femoris, vastus lateralis, and vastus medialis muscles, increased as quadriceps contracture progressed. However, the hardness value of the quadriceps muscles only increased in the period 1 week after immobilization. The serum creatinine phosphokinase level only increased in the period 2 weeks after immobilization. Therefore, we found that ultrasound shear wave elastography was a more accurate method to detect the pathophysiology of quadriceps contracture than measuring muscle hardness or serum creatinine phosphokinase levels.

Quadriceps contracture is defined as quadriceps atrophy, with muscle tissue replaced by fibrous tissue, resulting in muscle shortening [1,2]. In this study, for all periods of immobilization, decreased muscle size and length were observed. Our histological analysis showed that the atrophic changes included reductions in the cross-sectional area, minimum Feret's diameter, diameter, and perimeter of quadriceps muscle fiber as it progressed through 4 weeks of immobilization. Sarcomere length also decreased in all periods in the immobilization group. Our histological and morphological analyses showed that muscle fiber atrophy and muscle shortening result from quadriceps muscle contracture. These results were consistent with the previously reported characteristics of muscle contracture induced by muscle immobilization in the shortened position [35,36].

The mechanism of muscle fibrosis in muscle contracture is related to several factors that increase collagen production. These factors include *IL-1 β* and *TGF- β 1*. Previous research has shown that *IL-1 β* induces *TGF- β 1* synthesis via a *TGF- β* -dependent mechanism [37]. This induces fibroblast activation and collagen production [38]. *TGF- β 1* plays an important role in activating the differentiation of fibroblasts into myofibroblasts, a process related to muscle fibrosis [38,39]. In our study, the expression of *IL-1 β* and *TGF- β 1* mRNA in the immobilization group was higher than that in the control group. This result is similar to the trend reported from a previous study [36]. Another factor associated with fibrosis is hypoxia. The expression of *HIF-1 α* increases in fibrotic tissue and is related to hypoxia [40,41]. Hypoxia is stimulated by a decrease in the number of capillaries; this decrease is induced after immobilization for 4 weeks [42]. Honda et al. (2015) [36] showed that *HIF-1 α* mRNA expression increased 4 weeks after immobilization and promoted muscle fibrosis in cases of muscle contracture. In our research, we found that in the immobilization group, *HIF-1 α* mRNA expression was increased at 4 weeks after immobilization compared with 1, 2, or 3 weeks after immobilization. Previous research has also shown that α -SMA is related to the fibrosis mechanism [43]. α -SMA is a marker of myofibroblasts [44]. Myofibroblasts produce large quantities of collagen and are an important factor in pathological muscle contracture [45,46]. We found that the number of α -SMA positive cells in the immobilization group was increased at 1 week after immobilization. The overexpression of collagen types I and III in muscles, including in the perimysium, endomysium, and epithelium, is the main characteristic of muscle fibrosis in muscle contracture induced by immobilization [23,47]. In our study, the percentages of collagen types I and III also increased from 1 week after immobilization. We assume that muscle fibrosis in quadriceps contracture occurred during the early stages of immobilization (less than 2 weeks after immobilization), before progressing in the later stages of immobilization (3–4 weeks after immobilization). These results are similar to previously reported results [36]. Together, these results indicate that the upregulation of *IL-1 β* , *TGF- β 1*, and *HIF-1 α* mRNA affects the conversion of fibroblasts into myofibroblasts and induces collagen production, which is associated with the occurrence of quadriceps muscle contracture.

Gait assessment and palpation of quadriceps contracture are conventional assessment methods. Myogenic contractures occur after less than 2 weeks of joint immobilization, and muscle contractures with arthrogenic and myogenic changes occur after more than 4 weeks of joint immobilization [48]. Lameness due to quadriceps contracture occurs 3 to 5 weeks after injury [1]. When arthrogenic contracture occurs, the prognosis for treatment to return to normal function is poor [4].

A decreased range of motion in the stifle joint and a taut band around the cranial thigh muscle are the clinical signs of quadriceps contracture [1]. This can occur if the stifle joint is immobilized in the extension position for a long time [1,2]. In our study, we found that the range of stifle and ankle joint motion in the immobilization group decreased compared with that in the control group. These results are similar to those described in previous studies [1,3,4,23]. We assume that quadriceps muscle contracture was induced in all periods of the immobilization. The decreased stifle joint range of motion associated with progressive quadriceps contracture may be useful in detecting this condition. However, muscle properties cannot be objectively assessed.

Serum creatinine phosphokinase is another biomarker that can be used to diagnose muscle damage and myopathy [2,49]. Creatinine phosphokinase is an enzyme present in skeletal muscle tissue. When muscle is damaged, the enzyme leaks into the bloodstream [50]. However, a previous study of sartorius muscle contracture noted that there were no serum biochemical tests that are specific for muscle contracture [51]. In our research, we found that the level of serum creatinine phosphokinase only showed an increase at 2 weeks after immobilization, which means that it cannot be used to diagnose quadriceps contracture. The quadriceps contracture in this study was not due to muscle injury, but to abnormal shortening of the muscle–tendon unit induced by immobilization. Thus, it was suggested that serum creatinine phosphokinase levels do not increase after immobilization.

In recent years, it has been shown that imaging technologies can play a major role in the diagnosis of myopathies [17,52–55]. B-mode ultrasonography can be used to evaluate muscle atrophy and decreased muscle size [28]. In the present study, the quadriceps muscle thickness of the immobilized group was decreased. These results were consistent with the findings of muscle atrophy on histopathological examination. B-mode ultrasonography is a less invasive technique than histopathologic evaluation and can be used to assess muscle atrophy in the clinical practice.

Ultrasound shear wave elastography can evaluate muscle trauma and pathological changes in musculoskeletal tissue [17,55]. Although there have been reports of ultrasound elastography being used to assess muscle hardness and stiffness [56], there is a lack of information about the use of the technique to diagnose quadriceps contracture. Ultrasound shear wave elastography is a method that can be used to measure muscle stiffness and assess the changes in muscle elasticity that are characteristic of muscle contracture. In our study, we found there was a trend for quadriceps contracture lesions to have a high elasticity modulus and increased muscle stiffness when compared with pre-experimental data and the control group. The elastic modulus and muscle stiffness increased gradually with the progression of muscle contracture. Guo et al. (2018) [57] used ultrasound shear wave elastography to study three patients with gluteal muscle contracture and concluded that the elastic modulus of gluteal muscle with contracture is higher than that of the normal muscle. The increased elastic modulus, which indicates decreased muscle elasticity, was consistent with overexpression of collagen types I and III and increased expression levels of *IL-1 β* and *TGF- β 1* mRNA, suggesting muscle fibrosis associated with progressive muscle contracture. Therefore, ultrasound shear wave elastography is a diagnostic method that can assess muscle properties compared to joint range of motion and is less invasive than histopathology or gene expression level examination.

Tissue hardness meters can be used to detect muscle stiffness; however, their use in diagnosing quadriceps contracture is controversial. Niitsu et al. (2011) [8] reported that after exercise, muscles exhibit increased muscle hardness, which they measured using a tissue hardness meter. However, Akagi et al. (2015) [11] investigated neck and shoulder stiffness using both ultrasound elastography and a tissue hardness meter, but they found that the tissue hardness meter could not evaluate the muscle hardness level as well as ultrasound elastography. In our study, we found that the muscle hardness level increased only after 1 week in the immobilization group compared with that of the control group. Therefore, a tissue hardness meter cannot be used to detect quadriceps contracture. Decreased muscle elasticity is related to changes in the fibril arrangement in the endomysium as muscle contracture progresses [35]. Okita et al. (2004) [35] reported that collagen fibrils in the endomysium during muscle contracture were oriented in the circumferential direction at short sarcomere length. Consequently, based on quadriceps contracture pathogenesis involving the shortening of muscle length and decrease in muscle elasticity resulting in muscle stiffness, ultrasound shear wave elastography is more effective in quantifying muscle elasticity and muscle stiffness than a tissue hardness meter, which can only assess muscle stiffness.

Our study had several limitations. First, we did not evaluate the elastic modulus of the vastus intermedius muscle because this muscle is very small, and an ultrasound probe cannot access it. Second, the ultrasound elastography results were not compared with other imaging techniques, such as magnetic resonance imaging; this was because in this study we focused on diagnostic methods that can be easily accessed in clinical practice. Third, we only used male rats, in accordance with previous studies of muscle contracture [23]. It is unclear what effect sex hormones in the estrus cycle might have on the induction of muscle contracture, although it is known that estrogen and progesterone in the estrus cycle can affect muscle maintenance and increase muscle mass [58,59].

5. Conclusions

A diagnosis of quadriceps contracture can be obtained by palpating the muscle and assessing the gait status. In such cases, the disease has already advanced, and there is little chance of recovering muscle function. Furthermore, the level of serum creatinine phosphokinase and a tissue hardness meter cannot assess the pathogenesis of quadriceps contracture. The range of stifle joint motion can be used to evaluate quadriceps contracture, but it cannot provide objective assessments of muscle properties. Histopathology and expression levels of *IL-1 β* and *TGF- β 1* mRNA can assess the pathology and properties of the muscle but are more invasive techniques than ultrasound shear wave elastography. Shear wave elastography can be used to detect changes in muscle elasticity in quadriceps contracture after just 1 week of immobilization. Therefore, shear wave elastography is a potentially useful method for evaluating quadriceps contracture in the early stage. When the disease is diagnosed earlier and treatment started as soon as possible, the prognosis of quadriceps contracture is improved. Ultrasound shear wave elastography is expected to contribute to future research and have applications in clinical practice for early treatment and improving the prognosis of muscle contracture.

Author Contributions: Conceptualization, M.S. and K.S. (Kanokwan Suwankanit); methodology, M.S. and K.S. (Kanokwan Suwankanit); validation, M.S. and K.S. (Kanokwan Suwankanit); formal analysis, M.S., K.S. (Kanokwan Suwankanit), K.S. (Kazuhiko Suzuki) and M.K.; investigation, K.S. (Kanokwan Suwankanit); resources, M.S., K.S. (Kanokwan Suwankanit), K.S. (Kazuhiko Suzuki) and M.K.; data curation, M.S. and K.S. (Kanokwan Suwankanit); writing—original draft preparation, K.S. (Kanokwan Suwankanit); writing—review and editing, M.S.; visualization, M.S. and K.S. (Kanokwan Suwankanit); supervision, M.S.; project administration, M.S. and K.S. (Kanokwan Suwankanit); funding acquisition, K.S. (Kanokwan Suwankanit). All authors have read and agreed to the published version of the manuscript.

Funding: This research was funded by a grant from Mahidol University scholarship.

Institutional Review Board Statement: The animal study protocol was approved by the Ethics Committee of the Faculty of Agriculture, Tokyo University of Agriculture and Technology (R04-191; approval date: 26 October 2022).

Informed Consent Statement: Not applicable.

Data Availability Statement: The data presented in this study are available in article.

Acknowledgments: We would like to thank Akane Tanaka and Ryo Muko from the comparative animal medicine laboratory, Tokyo University of Agriculture and Technology for performing the histological procedures. We would also like to thank Ryou Tanaka from the veterinary surgery laboratory, Tokyo University of Agriculture and Technology, for the anesthesia machine and Kripitch Sutumaporn from the Veterinary Science Faculty, Mahidol University, for the histological interpretation.

Conflicts of Interest: The authors declare no conflict of interest. The funders had no role in the design of the study; in the collection, analyses, or interpretation of data; in the writing of the manuscript, or in the decision to publish the results.

References

1. Schulz, K.S. Management of muscle and tendon injury or disease. In *Small Animal Surgery Textbook*, 4th ed.; Fossum, T.W., Ed.; Elsevier Health Sciences: Philadelphia, PA, USA, 2013; pp. 1375–1390.
2. Canapp, S.O.; Deborah, G.S. Common conditions and physical rehabilitation of the athletic patient. In *Canine Rehabilitation and Physical Therapy*, 2nd ed.; Millis, D., David, L., Eds.; Elsevier's Health Sciences: Philadelphia, PA, USA, 2014; pp. 582–608.
3. Ulasan, S.; Captug-Ozdemir, O.; Gul-Sancak, I.; Bilgili, H. Treatment techniques of femoral quadriceps muscle contracture in ten dogs and two cats. *Kafkas Univ. Vet. Fak. Derg.* **2011**, *17*, 401–408.
4. Millis, D. Quadriceps contracture. In *Complications in Small Animal Surgery*, 1st ed.; Griffon, D., Hamaide, A., Eds.; John Wiley & Sons: Ames, IA, USA, 2016; pp. 692–696.
5. Taylor, J.; Tangner, C. Acquired muscle contractures in the dog and cat. A review of the literature and case report. *Vet. Comp. Orthop. Traumatol.* **2007**, *2*, 79–85.
6. Nichols, T.R.; Huyghues-Despointes, C.M. Muscular Stiffness. In *Encyclopedia of Neuroscience*; Binder, M.D., Hirokawa, N., Windhorst, U., Eds.; Springer Berlin Heidelberg: Berlin/Heidelberg, Germany, 2009; pp. 2515–2519. [[CrossRef](#)]

7. Oflaz, H.; Baran, O. A new medical device to measure a stiffness of soft materials. *Acta Bioeng. Biomech.* **2014**, *16*, 125–131. [PubMed]
8. Niitsu, M.; Michizaki, A.; Endo, A.; Takei, H.; Yanagisawa, O. Muscle hardness measurement by using ultrasound elastography: A feasibility study. *Acta Radiol.* **2011**, *52*, 99–105. [CrossRef] [PubMed]
9. Lee, Y.; Kim, M.; Lee, H. The measurement of stiffness for major muscles with shear wave elastography and myoton: A quantitative analysis study. *Diagnostics* **2021**, *11*, 524. [CrossRef]
10. Do, Y.; Lall, P.S.; Lee, H. Assessing the effects of aging on muscle stiffness using shear wave elastography and myotonometer. *Healthcare* **2021**, *9*, 1733. [CrossRef]
11. Akagi, R.; Kusama, S. Comparison between neck and shoulder stiffness determined by shear wave ultrasound elastography and a muscle hardness meter. *Ultrasound Med. Biol.* **2015**, *41*, 2266–2271. [CrossRef]
12. Bensamoun, S.F.; Ringleb, S.I.; Littrell, L.; Chen, Q.; Brennan, M.; Ehman, R.L.; An, K.N. Determination of thigh muscle stiffness using magnetic resonance elastography. *J. Magn. Reson. Imaging* **2006**, *23*, 242–247. [CrossRef]
13. Muraki, T.; Domire, Z.J.; McCullough, M.B.; Chen, Q.; An, K. Measurement of stiffness changes in immobilized muscle using magnetic resonance elastography. *Clin. Biomech.* **2010**, *25*, 499–503. [CrossRef]
14. Debernard, L.; Robert, L.; Charleux, F.; Bensamoun, S.F. A possible clinical tool to depict muscle elasticity mapping using magnetic resonance elastography. *Muscle Nerve* **2013**, *47*, 903–908. [CrossRef]
15. Low, G.; Kruse, S.A.; Lomas, D.J. General review of magnetic resonance elastography. *World. J. Radiol.* **2016**, *8*, 59–72. [CrossRef] [PubMed]
16. Ringleb, S.I.; Bensamoun, S.F.; Chen, Q.; Manduca, A.; An, K.N.; Ehman, R.L. Applications of magnetic resonance elastography to healthy and pathologic skeletal muscle. *J. Magn. Reson. Imaging* **2007**, *25*, 301–309. [CrossRef] [PubMed]
17. Klauser, A.S.; Miyamoto, H.; Bellmann-Weiler, R.; Feuchtner, G.M.; Wick, M.C.; Jaschke, W.R. Sonoelastography: Musculoskeletal applications. *Radiology* **2014**, *272*, 622–633. [CrossRef] [PubMed]
18. Inami, T.; Kawakami, Y. Assessment of individual muscle hardness and stiffness using ultrasound elastography. *J. Phys. Fitness. Sports. Med.* **2016**, *5*, 313–317. [CrossRef]
19. Shinohara, M.; Sabra, K.; Gennisson, J.L.; Fink, M.; Tanter, M. Real-time visualization of muscle stiffness distribution with ultrasound shear wave imaging during muscle contraction. *Muscle Nerve* **2010**, *42*, 438–441. [CrossRef] [PubMed]
20. Brandenburg, J.E.; Eby, S.F.; Song, P.; Zhao, H.; Brault, J.S.; Chen, S.; An, K. Ultrasound elastography: The new frontier in direct measurement of muscle stiffness. *Arch. Phys. Med. Rehabil.* **2014**, *95*, 2207–2219. [CrossRef] [PubMed]
21. Rominger, M.B.; Kälin, P.; Mastalerz, M.; Martini, K.; Klingmüller, V.; Sanabria, S.; Frauenfelder, T. Influencing factors of 2D shear wave elastography of the muscle—an ex vivo animal study. *Ultrasound Int. Open* **2018**, *4*, E54–E60. [CrossRef]
22. Drakonaki, E.; Allen, G.; Wilson, D. Ultrasound elastography for musculoskeletal applications. *Br. J. Radiol.* **2012**, *85*, 1435–1445. [CrossRef]
23. Suwankanit, K.; Shimizu, M. Rat Model of Quadriceps Contracture by Joint Immobilization. *Biology* **2022**, *11*, 1781. [CrossRef]
24. Onda, A.; Kono, H.; Jiao, Q.; Akimoto, T.; Miyamoto, T.; Sawada, Y.; Suzuki, K.; Kusakari, Y.; Minamisawa, S.; Fukubayashi, T. New mouse model of skeletal muscle atrophy using spiral wire immobilization. *Muscle Nerve* **2016**, *54*, 788–791. [CrossRef]
25. Jang, Y.; Park, Y.E.; Yun, C.-W.; Kim, D.-H.; Chung, H. The vest-collar as a rodent collar to prevent licking and scratching during experiments. *Lab. Anim.* **2016**, *50*, 296–304. [CrossRef] [PubMed]
26. Millis, D.; Levine, D. Joint motions and ranges. In *Canine Rehabilitation and Physical Therapy*, 2nd ed.; Millis, D., David, L., Eds.; Elsevier Health Sciences: Philadelphia, PA, USA, 2014; pp. 730–735.
27. Sakaeda, K.; Shimizu, M. Use of B-mode ultrasonography for measuring femoral muscle thickness in dogs. *J. Vet. Med. Sci.* **2016**, *78*, 803–810. [CrossRef] [PubMed]
28. Hida, T.; Ando, K.; Kobayashi, K.; Ito, K.; Tsushima, M.; Kobayakawa, T.; Morozumi, M.; Tanaka, S.; Machino, M.; Ota, K. Ultrasound measurement of thigh muscle thickness for assessment of sarcopenia. *Nagoya J. Med. Sci.* **2018**, *80*, 519–527. [PubMed]
29. Kudo, S.; Nakamura, S. Relationship between hardness and deformation of the vastus lateralis muscle during knee flexion using ultrasound imaging. *J. Bodyw. Mov. Ther.* **2017**, *21*, 549–553. [CrossRef] [PubMed]
30. Beeton, C.; Garcia, A.; Chandy, K.G. Drawing blood from rats through the saphenous vein and by cardiac puncture. *J. Vis. Exp.* **2007**, *7*, e266.
31. Method of Euthanasia. Available online: https://www.olac.berkeley.edu/sites/default/files/doc/adult_and_neonatal_mouse_and_rat_euthanasia.10.15.2020.pdf (accessed on 1 April 2022).
32. National Research Council (US). Committee for the Update of the Guide for the Care and Use of Laboratory Animals. In *Guide for the Care and Use of Laboratory Animals*, 8th ed.; National Academies Press: Washington, DC, USA, 2010.
33. Cardiff, R.D.; Miller, C.H.; Munn, R.J. *Manual Hematoxylin and Eosin Staining of Mouse Tissue Sections*; Cold Spring Harbor Laboratory Press: Cold Spring Harbor, NY, USA, 2014; pp. 655–658.
34. Livak, K.J.; Schmittgen, T.D. Analysis of relative gene expression data using real-time quantitative PCR and the $2^{-\Delta\Delta CT}$ method. *Methods* **2001**, *25*, 402–408. [CrossRef]
35. Okita, M.; Yoshimura, T.; Nakano, J.; Motomura, M.; Eguchi, K. Effects of reduced joint mobility on sarcomere length, collagen fibril arrangement in the endomysium, and hyaluronan in rat soleus muscle. *J. Muscle Res. Cell Motil.* **2004**, *25*, 159–166. [CrossRef]

36. Honda, Y.; Sakamoto, J.; Nakano, J.; Kataoka, H.; Sasabe, R.; Goto, K.; Tanaka, M.; Origuchi, T.; Yoshimura, T.; Okita, M. Upregulation of interleukin-1 β /transforming growth factor- β 1 and hypoxia relate to molecular mechanisms underlying immobilization-induced muscle contracture. *Muscle Nerve* **2015**, *52*, 419–427. [[CrossRef](#)]
37. Ismaeel, A.; Kim, J.-S.; Kirk, J.S.; Smith, R.S.; Bohannon, W.T.; Koutakis, P. Role of Transforming Growth Factor- β in Skeletal Muscle Fibrosis: A Review. *Int. J. Mol. Sci.* **2019**, *20*, 2446. [[CrossRef](#)]
38. Frangogiannis, N.G. Transforming growth factor- β in tissue fibrosis. *J. Exp. Med.* **2020**, *217*, e20190103. [[CrossRef](#)]
39. Sarrazy, V.; Billet, F.; Micallef, L.; Coulomb, B.; Desmoulière, A. Mechanisms of pathological scarring: Role of myofibroblasts and current developments. *Wound Repair. Regen.* **2011**, *19*, s10–s15. [[CrossRef](#)] [[PubMed](#)]
40. Tzouvelekis, A.; Harokopos, V.; Paparountas, T.; Oikonomou, N.; Chatziioannou, A.; Vilaras, G.; Tsiambas, E.; Karameris, A.; Bouros, D.; Aidinis, V. Comparative expression profiling in pulmonary fibrosis suggests a role of hypoxia-inducible factor-1 α in disease pathogenesis. *Am. J. Respir. Crit. Care Med.* **2007**, *176*, 1108–1119. [[CrossRef](#)] [[PubMed](#)]
41. Haase, V.H. Hypoxia-inducible factors in the kidney. *Am. J. Physiol. Renal Physiol.* **2006**, *291*, F271–F281. [[CrossRef](#)] [[PubMed](#)]
42. Matsumoto, Y.; Nakano, J.; Oga, S.; Kataoka, H.; Honda, Y.; Sakamoto, J.; Okita, M. The non-thermal effects of pulsed ultrasound irradiation on the development of disuse muscle atrophy in rat gastrocnemius muscle. *Ultrasound. Med. Biol.* **2014**, *40*, 1578–1586. [[CrossRef](#)] [[PubMed](#)]
43. Rao, B.; Malathi, N.; Narashiman, S.; Rajan, S.T. Evaluation of myofibroblasts by expression of alpha smooth muscle actin: A marker in fibrosis, dysplasia and carcinoma. *J. Clin. Diagnostic Res.* **2014**, *8*, ZC14–ZC17.
44. Hinz, B. Myofibroblasts. *Exp. Eye Res.* **2016**, *142*, 56–70. [[CrossRef](#)]
45. Abdel, M.P.; Morrey, M.E.; Barlow, J.D.; Kreofsky, C.R.; An, K.N.; Steinmann, S.P.; Morrey, B.F.; Sanchez-Sotelo, J. Myofibroblast cells are preferentially expressed early in a rabbit model of joint contracture. *J. Orthop. Res.* **2012**, *30*, 713–719. [[CrossRef](#)]
46. Phan, S.H. Biology of fibroblasts and myofibroblasts. *Proc. Am. Thorac. Soc.* **2008**, *5*, 334–337. [[CrossRef](#)]
47. Wang, F.; Zhang, Q.-B.; Zhou, Y.; Chen, S.; Huang, P.-P.; Liu, Y.; Xu, Y.-H. The mechanisms and treatments of muscular pathological changes in immobilization-induced joint contracture: A literature review. *Chin. J. Traumatol.* **2019**, *22*, 93–98. [[CrossRef](#)]
48. Trudel, G.; Uhthoff, H.K. Contractures secondary to immobility: Is the restriction articular or muscular? An experimental longitudinal study in the rat knee. *Arch. Phys. Med. Rehabil.* **2000**, *81*, 6–13. [[CrossRef](#)]
49. Robert, L.H.; Bender, H.S. Muscle. In *Duncan and Prasse's Veterinary Laboratory Medicine: Clinical Pathology*, 5th ed.; Latimer, K.S., Ed.; John Wiley & Sons: West Sussex, UK, 2011; pp. 283–294.
50. Aujla, R.S.; Patel, R. *Creatine Phosphokinase*; StatPearls Publishing: Treasure Island, FL, USA, 2022.
51. Spadari, A.; Spinella, G.; Morini, M.; Romagnoli, N.; Valentini, S. Sartorius muscle contracture in a German shepherd dog. *Vet. Surg.* **2008**, *37*, 149–152. [[CrossRef](#)] [[PubMed](#)]
52. Zimmer, M.; Kleiser, B.; Marquetand, J.; Ates, F. Characterization of muscle weakness due to myasthenia gravis using shear wave elastography. *Diagnostics* **2023**, *13*, 1108. [[CrossRef](#)] [[PubMed](#)]
53. Cebula, A.; Cebula, M.; Kopyta, I. Muscle Ultrasonographic Elastography in Children: Review of the Current Knowledge and Application. *Children* **2021**, *8*, 1042. [[CrossRef](#)] [[PubMed](#)]
54. Wen, J.; Wang, Y.; Jiang, W.; Luo, Y.; Peng, J.; Chen, M.; Jing, X. Quantitative evaluation of denervated muscle atrophy with shear wave ultrasound elastography and a comparison with the histopathologic parameters in an animal model. *Ultrasound Med. Biol.* **2018**, *44*, 458–466. [[CrossRef](#)] [[PubMed](#)]
55. Lv, H.; Li, Z.; Hu, T.; Wang, Y.; Wu, J.; Li, Y. The shear wave elastic modulus and the increased nuclear factor kappa B (NF- κ B/p65) and cyclooxygenase-2 (COX-2) expression in the area of myofascial trigger points activated in a rat model by blunt trauma to the vastus medialis. *J. Biomech.* **2018**, *66*, 44–50. [[CrossRef](#)] [[PubMed](#)]
56. Cimmino, M.A.; Grassi, W. What is new in ultrasound and magnetic resonance imaging for musculoskeletal disorders? *Best. Pract. Res. Clin. Rheumatol.* **2008**, *22*, 1141–1148. [[CrossRef](#)]
57. Guo, R.; Xiang, X.; Qiu, L. Shear-wave elastography assessment of gluteal muscle contracture: Three case reports. *Medicine* **2018**, *97*, e13071. [[CrossRef](#)]
58. Carson, J.A.; Manolagas, S.C. Effects of sex steroids on bones and muscles: Similarities, parallels, and putative interactions in health and disease. *Bone* **2015**, *80*, 67–78. [[CrossRef](#)]
59. Rosa-Caldwell, M.E.; Greene, N.P. Muscle metabolism and atrophy: Let's talk about sex. *Biol. Sex Differ.* **2019**, *10*, 43. [[CrossRef](#)]

Disclaimer/Publisher's Note: The statements, opinions and data contained in all publications are solely those of the individual author(s) and contributor(s) and not of MDPI and/or the editor(s). MDPI and/or the editor(s) disclaim responsibility for any injury to people or property resulting from any ideas, methods, instructions or products referred to in the content.